NJC

Accepted Manuscript

ROYAL SOCIETY OF CHEMISTRY

www.rsc.org/njc

A thermodynamic picture is reported for cys-Pb^{2+}, psh-Pb^{2+}, gsh-Pb^{2+}, gsh-Zn^{2+}systems, and equilibrium constants can be predicted for any experimental condition

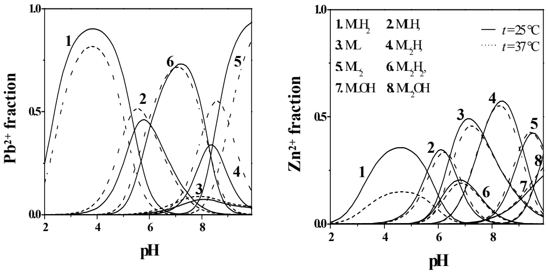

Submitted to: *New J. Chem*

Thermodynamic data for Pb^{2+} and Zn^{2+} sequestration by biologically important S-donor ligands, at different temperatures and ionic strengths

Francesco Crea,[a] **Gabriella Falcone,**[a] **Claudia Foti,**[a]* **Ottavia Giuffrè**[a] **and Stefano Materazzi**[b]

[a] *Dipartimento di Scienze Chimiche, Università di Messina, Viale F. Stagno d'Alcontres 31, 98166 Messina, Italy*
[b] *Dipartimento di Chimica, Università "La Sapienza", p.le A. Moro 5, 00185 Roma, Italy*

Thermodynamic parameters for the interactions of cysteine (*cys*) and penicillamine (*psh*) with Pb(II), and of glutathione (*gsh*) with Pb(II) and Zn(II) were determined in $NaNO_3$ or NaCl aqueous solution by potentiometry, at different ionic strengths ($0 < I \leq 1$ mol L^{-1}) and temperatures ($15 \leq t \leq 45$ °C). For Pb^{2+} systems, the formation of PbL, PbLH, $PbLH_2$ and PbL_2 species was found, together with PbLOH for c*ys* and *psh*, and PbL_2H and PbL_2H_2 for *gsh*. The speciation models for Pb^{2+} -*psh* and -*gsh* systems were confirmed by UV spectrophotometric measurements. For Zn^{2+}-*gsh* system, a more complex speciation model was obtained with the formation of ZnL, ZnLH, $ZnLH_2$, ZnL_2, ZnL_2H, ZnL_2H_2, ZnLOH and ZnL_2OH species. From the dependence on temperature of formation constants, rough ΔH values were evaluated: the main contribution to the complexation free energy is entropic in nature, with small enthalpic values. Moreover, from the dependence on ionic strength, formation constants extrapolated at $I = 0$ mol·L^{-1} were obtained.

The sequestering ability of the ligands towards Pb^{2+} and Zn^{2+} was evaluated by determining the $pL_{0.5}$, *i.e.* the -log of the concentration of the ligand able to complex half of the metal ion fraction. All these ligands show good sequestering ability. For Pb^{2+}-*cys*, -*psh* and -*gsh* systems, $pL_{0.5}$ reaches the value of 8.2, 9.0 and 5.9, respectively, at pH = 7, $I = 0.1$ mol L^{-1} and $t = 25$ °C. At the same experimental conditions, the sequestering ability of *gsh* towards Zn^{2+} is lower, with $pL_{0.5} = 4.1$.

Introduction

Sulfur containing compounds are found in all body cells and are indispensable for life owing the key roles in many biological processes. Sulfhydryl group forms thioester linkages that are necessary for the activation of molecules such as acetate; moreover it is

---

[*] Corresponding author: Claudia Foti: email address: cfoti@unime.it; fax +39 090392827

important in the iron containing flavoenzymes and it is responsible, in cysteine, for the major covalent cross-links in protein structures, owing to its ability to form inter- and intrachain disulfide bonds with other cysteine residues.[1-3] The sulfhydryl group of proteins or polypeptides represents the most important site for binding of many metal ions. The metals replace H or they form chelates. In this way, the protein structure is altered considerably and no disulfide bridges can be formed.

The importance of sulfur compounds is also due to their therapeutical use.[4] They are used in diets for patients with AIDS, because of increased risk of sulfur-containing aminoacid deficiency, but also in a number of oxidative stress models (such as ischemia-reperfusion injury, diabetes, cataract formation) or as chelating agents in acute poisoning of heavy metals.

Literature thermodynamic data on S-donor ligands are significantly less numerous than those on N- and O- donor ones.[5-7] For this reason, in recent years we have undertaken a detailed study on the acid-base and binding properties of S-donor ligands against some metal and organometallic cations of environmental and biological relevance.[8-16] Here we extended the study to the interaction of some sulfur containing aminoacids (see Fig. 1) towards a toxic metal, such us Pb^{2+}, and an essential metal, such as Zn^{2+}, recently studied by thermogravimetric analysis.[17]

It is well known that amino carboxylic acid acts as negatively charged chelating ligand toward metal ions, by coordinating both through the $-NH_2$ and the $-COO^-$ groups,[18, 19] whereas, only spare information[5-7] is available on the donor ability of sulfur-containing amino acid, in which the sulfur atom is also a possible coordinating site. Amino acids here taken in account are cysteine and penicillamine together with glutathione, a cysteine-containing tripeptide.

Cysteine is a major metal binding site in proteins. Penicillamine, a degradation product of penicillin, finds use as a therapeutic chelating agent. Glutathione is a major component of the cellular antioxidant system and plays an important role in the detoxification of xenobiotic compounds and in the antioxidation of free radicals.

Cysteine and penicillamine contain three dissociable protons each. As results of the presence of the three complex-forming functional groups, *cys* and *psh* are tipically ambidentate ligands. The possible metal binding sites are different in nature: COO^- is rather hard, S is fairly soft and NH_2 is borderline.

The thermodynamic parameters for the interactions of *cys*, *psh* and *gsh* with Hg^{2+}, CH_3Hg^+, $(CH_3)_2Sn^{2+}$, $(CH_3)_3Sn^+$, $(C_2H_5)_3Sn^+$ and $(C_3H_7)_3Sn^+$ were determined in our recent papers.[8-15] Here, we extend the study to the interactions with Pb^{2+} and Zn^{2+}: these systems have not been widely studied and the only literature thermodynamic data are resumed in Table 1.[5, 6, 20-26] The purpose was to define the speciation models (*i.e.* "its distribution among defined chemical species in a system"[27]) and to give a complete picture of the thermodynamic properties of these systems, defining also the dependence on the ionic strength and the temperature, previously not taken into account. This will give the opportunity to evaluate and predict the distribution of species in any experimental condition. Moreover, it must be remembered that the knowledge of the speciation of an element is the basis of biological studies, since it influences the availability, the solubility, the cell membrane permeability and the toxicity of the element itself.

Studies on Pb^{2+} and Zn^{2+} were performed in $NaNO_3$ or NaCl by potentiometry, at different ionic strength values ($0 < I \leq 1$ mol L^{-1}) and temperatures ($15 \leq t \leq 45$ °C). On the basis of potentiometric results, the equilibrium behaviour and the speciation model in a wide pH range will be discussed. In addition UV measurements were carried out in order to confirm the potentiometric findings. On the basis of the speciation models and the formation constant values reported, the sequestering ability of *cys*, *psh* and *gsh* ligands towards Pb(II) and Zn(II) cations was quantitatively evaluated.

Experimental

Materials

$Pb(NO_3)_2$ and $ZnCl_2$ salts were supplied by Fluka and Riedel-de-Haen respectively. The ligands [L-cysteine (H_2*cys*), D,L-penicillamine (H_2*psh*) and glutathione reduced (H_3*gsh*)] were supplied by Fluka or Aldrich. Their purity was controlled by potenziometry and resulted > 99.5%. They were therefore used without further purification. The sodium chloride and sodium nitrate salts (Aldrich, puriss.), previously dried at 110 °C, was used to prepare the corresponding solution by weighing. The concentrated ampoules of hydrochloric acid and sodium hydroxide (Fluka) were used to prepare the corresponding diluted solutions. The solutions of hydrochloric acid were standardised against sodium carbonate, those of sodium hydroxide against potassium hydrogen phthalate. All solutions were protected from atmospheric CO_2 using soda lime traps. Grade A glassware and twice-distilled water were employed in the preparation of all solutions.

Potentiometric equipment and procedure

The potentiometric titrations were performed independently by two operators using different reagents and different systems in order to minimise systematic errors. The equipments used were the 809 Metrohm *Titrando* apparatus equipped with a combined glass electrode (Ross type 8102, from Thermo/Orion) or with a half cell glass electrode (Ross type 8101, from Thermo/Orion); in this last case, a double junction reference electrode (type 900200, from Thermo/Orion) was used. The estimated reproducibility was ±0.15 mV and ±0.003 mL for the e.m.f. and titrant volume readings, respectively. The apparatus were connected to a PC, and automatic titrations were performed using the Metrohm *TiAMO* 1.0 software to control titrant delivery, data acquisition and to check for e.m.f. stability. The measurement cells were thermostated at the prefixed temperature (±0.1)K by means of water circulation from a thermocryostat (mod. D1-G Haake). Independent experiments were performed at least three times.

For Pb^{2+}-L systems (L = H_2cys, H_2psh, H_3gsh), the potentiometric measurements were carried out by titrating solutions containing different amounts of ligand ($0.5 \leq C_L \leq 2$ $mmol\cdot L^{-1}$) and the metal cation ($C_{Pb} = 0.5$ $mmol\cdot L^{-1}$) to obtain a concentration C_{Pb}/C_L ratios ranging from 0.25 to 1, $NaNO_3$ to fix the ionic strength to a predetermined value ($0 < I \leq 1$ $mol\cdot L^{-1}$), nitric acid to have the fully protonated form of the ligands. A volume of 25 ml of each solution was titrated with standard sodium hydroxide in the pH range 2.5 to 10.5. The upper limit was chosen within the range for reliable pH measurements of glass membrane electrode. The same procedure, and the same pH range, was used for Zn^{2+}-gsh^{3-} system, by using NaCl as ionic medium and the following concentration range: $2.5 \leq C_{gsh} \leq 10$ $mmol\cdot L^{-1}$, $2.5 \leq C_{Zn} \leq 5$ $mmol\cdot L^{-1}$, $0.5 \leq C_{Zn}/C_L \leq 1$, $0.1 \leq C_{NaCl} \leq 1$ $mol\cdot L^{-1}$. For each experiment, independent titrations of HCl with NaOH standard solutions were performed in the same experimental conditions of temperature and ionic strength as the systems under study in order to determine the formal electrode potential. The free hydrogen ion concentration scale was used (pH = -log[H^+]). The reliability of the calibration in the alkaline range was checked by calculating the pK_w values. For each measurement, 80-100 data points were collected, and the equilibrium state during titrations was checked by adopting some usual precautions, such as checking the time required to reach equilibrium and performing back titrations. Pure nitrogen was bubbled through the solutions in the titration cells in order to avoid O_2 and CO_2 inside and the solutions were magnetically stirred.

Spectrophotometric equipment and procedure

The spectrophotometric measurements were carried out using a Varian Cary 50 UV-VIS spectrophotometer equipped with an optic fiber probe with a fixed 1 cm path length; preliminary absorbing spectra were recorded in order to know the wavelength interval where the ligands absorb ($210 \leq \lambda \leq 320$ nm). The spectrophotometer was connected to a PC and the acquisition of the couple of data absorbance (A) vs. wavelength (λ, nm) was made by the Varian Cary WinUV (version 3.00) software. During these measurements, in the thermostatted measurement cell, a combined glass electrode (Ross type 8102, from Thermo/Orion) connected to a Metrohm 713 potentiometer was introduced. The combined glass electrode was standardized before each experiment in terms of pH = -log[H^+], as reported in the previous Section. In this order, we were able to record simultaneously the couple of data A vs. λ (nm), and e.m.f. (mV) vs. volume of titrant (mL). The titrant was delivered in the measurement cell by means of a 665 Metrohm automatic burette, and the homogeneity of the solutions during the titration was performed with a stirring bar. Before each experiment, N_2(g) was bubbled in the solutions for at least 5 min in order to exclude the presence of CO_2(g) and O_2(g).

The spectrophotometric measurements were carried out on Pb^{2+}-L systems (L = H_2*cys*, H_2*psh*, H_3*gsh*), by titrating solutions containing different amounts of the ligand ($0.1 \leq C_L \leq 0.3$ mmol L^{-1}) and the metal ($0.1 \leq C_{Pb} \leq 0.3$ mmol L^{-1}) under study, at different metal-ligand concentration ratios ($0.5 \leq C_M/C_L \leq 1$ mmolL^{-1}) in a wide pH range values ($2 \leq pH \leq 10$). Small increments of standard NaOH solution were added to each solution in order to obtain the maximum absorbance of each predominant species, according to the speciation diagrams of the systems.

Calculations

Several computer programs were used: 1) BSTAC and STACO[28] for the refinement of the parameters of the acid-base titrations (such as the analytical concentration of the reagent and E^0) and the calculation of the formation constants of the complexes; 2) HYSPEC[29] for the analysis of UV spectra; 3) HYSS[30] for the calculation of conditional formation constants; 4) ES4ECI[28] to calculate formation percentages of the species and to plot speciation diagrams; 5) LIANA[28] for the fitting of the linear and nonlinear equations for the ionic strength dependence of the formation constants.

Results

Speciation profile

Calculations on metal-ligand interactions were performed by considering the thermodynamic parameters concerning both the protonation of the ligands and the hydrolysis of the metal cations. The literature equilibrium constants used in this work for the protonation of *cys*, *psh* and *gsh* and the hydrolysis of Pb^{2+} and Zn^{2+}, at the same ionic strength values of the experimental measurements on metal-ligand systems,[10-12, 31, 32] are reported in Table 2.

Taking into account the above mentioned species, several trials were performed on the experimental potentiometric data, considering different sets of complex species, in order to find the best speciation model. The selected speciation models are those which had the best statistical fit,[33] without giving systematic drifts in the residuals.

Cys^{2-} and *psh*$^{2-}$ behave similarly in presence of Pb^{2+}, with the formation of PbL^0, $PbLH^+$, $PbLH_2^{2+}$, $PbL(OH)^-$ and PbL_2^{2-} species. Experimental formation constants are reported in Table 3 at three ionic strength values, i.e. I = 0.1, 0.5 and 1 mol L^{-1} ($NaNO_3$). Stability of several Pb^{2+}-*cys*$^{2-}$ and Pb^{2+}-*psh*$^{2-}$ species is very similar, with, as an example log β = 13.12 and 13.37 for the formation of Pb(*cys*)^0 and Pb(*psh*)^0, at I = 0.1 mol L^{-1}. Distribution of species is shown in Fig. 2(a)-(b): as can be observed, in the pH range of interest for biological and natural fluids ($5 \leq pH \leq 8$), the main species is PbL^0, which almost all of the metal fraction present under this form. At pH > 8, there is the coexistence of PbL_2^{2-} and $PbL(OH)^-$, while the mono- and di- protonated $PbLH^+$ and $PbLH_2^{2+}$ species are formed only at pH < 5.

In the presence of *gsh*$^{3-}$, the speciation of Pb^{2+} is slightly more complex with the formation of 1:1 and 1:2 species: Pb(*gsh*)$^-$, Pb(*gsh*)H^0, Pb(*gsh*)H_2^+, Pb(*gsh*)$_2^{4-}$, Pb(*gsh*)$_2$H^{3-} and Pb(*gsh*)$_2H_2^{2-}$. The speciation model, together with the formation constant values, is reported in Table 3. Stability of species is lower respect to those of *cys* and *psh*, with log β = 13.37, 13.12 and 9.67 for the formation of Pb(*psh*)^0, Pb(*cys*)^0 and Pb(*gsh*)$^-$, respectively. The coordination mode was not studied here, but some consideration can be made by analogy with other metals. In fact, the trend of stability is in agreement with that observed in recent papers[12, 13] concerning the interactions of *cys*, *psh* and *gsh* with Hg^{2+} and CH_3Hg^+ cations. Stability of *gsh* species was always lower respect to those of two other S-donor ligands. As an example, logβ(HgL) = 34.54, 34.24, 32.31, and logβ(CH_3HgL) = 17.29, 16.82, 15.98, for *cys*, *psh* and *gsh*, respectively. Results were supported by ^1H NMR and, for CH_3Hg^+ systems, by also ESI-MS and MS/MS studies. These techniques suggested that the functional group of *gsh* much more involved in the coordination of both Hg^{2+} and CH_3Hg^+ is the thiolic one, on the whole pH range studied. For *cys*$^{2-}$ and *psh*$^{2-}$ systems, ^1H NMR and ESI MS measurements evidenced the presence of $S \rightarrow Hg$ and $O \rightarrow Hg$ coordination.

The distribution diagram in Fig. 2(c) shows the relevance of Pb^{2+}-*gsh*$^{3-}$ species over a wide pH range: in particular, metal fraction values greater than 0.7 can be observed for Pb(*gsh*)H_2^+ at pH ~ 4, for Pb(*gsh*)$_2H_2^{2-}$ at pH ~ 7 and for Pb(*gsh*)$_2^{4-}$ at pH > 10. Pb(*gsh*)H^0 and Pb(*gsh*)$_2$H^{3-} reach 0.5 of metal fraction at pH ~ 6 and pH ~ 9, respectively.

As concerns the Zn^{2+}-*gsh*$^{3-}$ system, analysis of potentiometric measurements evidenced the formation of species with the same stoichiometry of those with Pb^{2+} (*i.e.*, Zn(*gsh*)$^-$, Zn(gsh)H^0, Zn(gsh)H$_2^+$, Zn(gsh)$_2^{4-}$, Zn(gsh)$_2$H^{3-} and Zn(gsh)$_2$H$_2^{2-}$), together with the two mixed hydrolytic Zn(gsh)OH^{3-} and Zn(gsh)$_2$OH^{5-}. In the pH range of interest for biological fluids ($5 \leq pH \leq 8$), the main species are Zn(gsh)H^0, Zn(gsh)$_2^{4-}$ and Zn(gsh)$_2$H^{3-}, which reach respectively the 0.3, 0.5 and 0.6 of the metal fraction, as can be observed in the speciation diagram reported in Fig. 3.

Dependence on ionic strength and temperature

In order to have a complete picture of the thermodynamic parameters of these systems, experimental measurements were performed at different ionic strength values and, for Pb^{2+}-gsh^{3-} and Zn^{2+}-gsh^{3-} systems, at different temperatures.

The dependence on ionic strength was taken into account by the Debye-Hückel type equation:[34-36]

$$\log\beta = \log\beta^0 - 0.51 \cdot z^* \frac{\sqrt{I}}{1+1.5\sqrt{I}} + C\,I \qquad (1)$$

where $z^* = \Sigma\,(\text{charges})^2_{\text{reactants}} - \Sigma\,(\text{charges})^2_{\text{products}}$, β is the formation constant, β^0 is the formation constant at infinite dilution. C is an empirical parameter that depends on the charges involved in the formation reaction. By equation (1) and equilibrium constants at different ionic strengths of Table 3, we obtained the values of formation constants extrapolated at $I = 0$ mol·L^{-1}, together with the empirical C parameter reported in Table 4. Values are referred to NaNO$_3$ as ionic medium for Pb^{2+} systems and to NaCl for Zn^{2+} system. NaCl was chosen since it is one of the main ionic component of natural and biological fluids. For the study of Pb^{2+} systems, NaCl was substituted by NaNO$_3$ in order to prevent the complexing action of Cl$^-$ towards the metal cation.

In many papers we evidenced the dependence of the C empirical parameter on the charges involved in the formation reaction (z*), and some ligand classes showed constant value of C/z*.[10, 13, 37] Data reported in Table 4 show a significant dispersion, but it was possible to derive a linear dependence from z* with: $C = 0.72(\pm0.04) - 0.11(\pm0.02)\,z^*$, for Pb^{2+} systems, and $C = -1.7(\pm0.3) + 0.14(\pm0.02)\,z^*$, for Zn^{2+}. These equations can be used for a fairly good predictive value for other ligands of this class.

Experimental measurements on Pb^{2+}- and Zn^{2+}- gsh systems were performed at different temperatures in the range $15 \leq t \leq 45$ °C (at $I = 0.1$ mol L^{-1}). Experimental values are reported in Table 5. Pb^{2+} system shows a higher dependence on temperature, with respect to Zn^{2+}. As an example, the logβ values vary from 10.14 (at t = 15 °C) to 8.82 (at t = 37 °C), for Pb(gsh)^0, and from 8.90 (at t = 15 °C) to 8.74 (at t = 37 °C), for Zn(gsh)^0. This is evident also from the distribution diagrams reported at two different temperature in Fig. 4. Increasing the temperature from 25 to 37 °C, more significant changes can be observed in the distribution of some species of Pb^{2+}, while those relating to Zn^{2+} are negligible, except for Zn(*gsh*)H_2^+.

Formation constants at different temperatures allowed us to calculate the enthalpy values by applying the van't Hoff equation (assuming negligible the contribution of ΔC_p in a small temperature range). Results are reported in Table 6, together with the overall free energy and the entropy changes determined by taking into account the stability constants obtained from potentiometric measurements. Table 6 also contains the thermodynamic parameters calculated according to the most probable formation reaction. For both systems, if we consider the partial formation reactions, the main contribution to the complexation free energy is entropic, with small enthalpic values. The only exception is for Pb(*gsh*)$^-$ formation, for which an exothermic value of enthalpy was obtained, with small entropic values.

The knowledge of the parameters for the dependence on the ionic strength and temperature gives a complete thermodynamic picture of these systems, whose equilibrium constants can therefore be predicted for any experimental condition.

Spectrophotometric properties

UV investigations were used to confirm the speciation model for Pb^{2+} -*psh* and -*gsh* systems and to determine the spectroscopic properties of the species, such as in several previous papers.[9, 10, 13, 38, 39] Measurements were performed in the spectral range $210 \leq \lambda \leq 320$ nm, in which preliminary tests revealed that Pb^{2+} solutions do not absorb, while the molar absorbance spectra of protonated and unprotonated species of the ligands have previously been calculated[13] and are shown in Fig. 5.

The analysis of A *vs.* λ data, by HYSPEC program,[29] confirms the speciation models obtained by potentiometric measurements, for both Pb^{2+} -*psh* and -*gsh* systems. For the analysis of UV spectrophotometric data, we chose to calculate the conditional formation constants,[30] as defined by Schwarzenbach.[40] This choice comes from the collinearity problems bound to the least squares calculations of stability constants using A *vs.* λ data at various pH values; differences in the values of β obtained by these two different techniques are cancelled by calculating conditional constants, and this is particularly true when dealing with complicate systems (number of complex species > 2). Table 7 reports the conditional formation constants in the pH range of interest for natural and biological fluids ($5 \leq pH \leq 8.5$), calculated by using potentiometric and spectrophotometric data. A good agreement was obtained, as can also be observed in Fig. 6, where the linear correlation between the two set of data is shown (r = 0.99).

At the same time, it was possible to define the UV spectral properties of these systems, *i.e.* to calculate the molar absorbance spectra of the complex species. These values are shown in Fig. 5. All Pb^{2+}-*psh* species show a maximum at λ = 210 nm. The molar extinction coefficients vary from ε = 13049±2400 L mol^{-1} cm^{-1}, for MLOH, to 150890±11000 L mol^{-1} cm^{-1}, for ML_2. A second maximum at λ = 266 nm was observed for ML, MLH and MLOH species, with ε = 4249±210, 16202±2200 and 4317±46 L mol^{-1} cm^{-1}, respectively.

For Pb^{2+}-*gsh* species, the maximum molar extinction coefficients at λ = 210 nm vary from 13750±2800 L mol^{-1} cm^{-1} , for MLH, to 69703±3100 L mol^{-1} cm^{-1} for ML_2H_2. A second maximum was observed at λ = 263 nm for ML and ML_2 (ε = 5228±88 and 8568±220 L mol^{-1} cm^{-1}, respectively), and at λ = 267 nm for MLH (ε = 3927±110 L mol^{-1} cm^{-1}).

Sequestering ability

The analysis of the stability constant values of metal-ligand complexes is not sufficient to assess the global binding ability of the ligand towards the metal cation, since different factors can influence the formation yields of the species: the hydrolysis of the metal, the protonation of the ligand, the interactions with other components. To make fast and reliable the quantification of the sequestering ability of a ligand toward a given component, in the last years our research group started to use the semiempirical parameter $pL_{0.5}$.[8,10-13,41] This parameter represents the total ligand concentration necessary to sequester 50% of a given metal ion present as trace in given conditions, even in the presence of other components. Higher is the $pL_{0.5}$ values, higher is the sequestering ability.

The value of $pL_{0.5}$ can be calculated by plotting the mole fraction (x) of the metal cation (present in trace) complexed by the ligand as a function of pL (pL = -log $[L]_{tot}$, $[L]_{tot}$ = total ligand concentration). Since this function is represented by a sigmoid curve, which rapidly increases over a relatively small change in concentration, a Boltzmann type equation (which tends asymptotically to 1 for pL→ ∞ and to 0 for pL→ 0) can be used:

$$x = \frac{1}{1+10^{(pL - pL_{0.5})}} \qquad (2)$$

The sum of mole fraction of Pb^{2+} and Zn^{2+} complexed by *cys*, *psh* and *gsh* is shown in Figs 7-9, in some experimental condition chosen as examples. Fig. 7 reports a comparison of different Pb^{2+} systems, at the same experimental condition, *i.e.* I = 0.1 mol L^{-1}, t = 25 °C and pH = 7. Penicilamine shows the higher sequestering ability towards Pb^{2+}, with $pL_{0.5}$ = 9.0, 8.2 and 5.9 for *psh*, *cys* and *gsh*, respectively. The same trend can be observed towards Zn^{2+} ($pL_{0.5}$ = 7.2, 5.7 and 4.7 for *psh*, *cys* and *gsh*, respectively). Figs. 8 and 9 report the effect of experimental conditions on the sequestering ability of glutathione. While the influence of temperature is not particularly marked for both metal cations, significant is the effect of the ionic strength and of pH. For Pb^{2+}-*gsh* system, the values vary from $pL_{0.5}$ = 5.9 (I = 0.1 mol L^{-1}, t = 25 °C, pH = 7), to 4.3 (I = 1 mol L^{-1}, t = 25 °C, pH = 7), to 4.2 (I = 0.1 mol L^{-1}, t = 25 °C, pH = 5). Greater are the variation for Zn^{2+}-*gsh* system, with $pL_{0.5}$ that drastically decreases from 5.1 (I = 0.1 mol L^{-1}, t = 37 °C, pH = 7) to 2.7 (I = 0.1 mol L^{-1}, t = 25 °C, pH = 5). The calculated values of $pL_{0.5}$ are resumed in Table 8, together with those, for comparison, towards other metal and organometallic cations previously determined.[10-13] As can be seen, sequestering ability of S-donor ligands towards Pb^{2+} and Zn^{2+} is significantly lower with respect to those towards Hg^{2+} and CH_3Hg^+, while is higher with respect to those of alkyltin cations. In particular, for *gsh*, the $pL_{0.5}$ values follow the trend: $Hg^{2+} >> CH_3Hg^+ >> Pb^{2+} > Zn^{2+} > (CH_3)_2Sn^{2+} > (CH_3)_3Sn^+$.

Comparison with literature data

As pointed out in the Introduction, not many thermodynamic data are reported in the literature on Pb^{2+}- and Zn^{2+}- *S*-donor ligand interaction.[5, 6, 20-26] In particular, it should highlight the lack of studies at variable ionic strength and temperature. Most of data are referred at 25 °C and at I = 0.1 or 3 mol L^{-1}.

The most comprehensive studies are those of Williams and *coworkers*,[20-22, 26] who systematically analyzed the thermodynamic properties of the systems here considered. As concerns Pb^{2+} systems, our speciation models are quite in agreement with those of Williams, which provide for the formation of PbL, PbLH, PbL_2, PbL_2H, $PbL_2(OH)$ and, for *gsh* only, PbL_2H_2 species. In addition we considered the $PbLH_2$ species, the formation of which takes place in the pH range not investigated by Williams (2 < pH < 4.5). Also for Zn^{2+}-*gsh* system, there is agreement with Williams model,[26] except for $ZnLH_2$ species, for which the same considerations on Pb^{2+} systems can be done.

Recently, Ferretti *et al.*[23] reported a detailed study on Zn^{2+}-*gsh* interactions. They tested different speciation models taking also into account the formation of many dinuclear species. On the basis of potentiometric, ^1H NMR and ESI mass spectrometric results, they finally supported a speciation model with ZnL, ZnLH, ZnL_2, ZnL_2H, ZnL_2H_2, ZnL_2OH, $ZnL_2(OH)_2$, Zn_2L_2OH and $Zn_2L_2(OH)_2$. In part, the differences with our model can probably be attributed to the pH range considered. The $ZnL_2(OH)_2$ species, not reported by us, reaches significant percentages of formation beyond pH 10.5 (we experimentally reached pH = 10.5). But, the difference between the two models can be accounted for the presence of hydrolytic equilibria which may complicate the data treatmen. The hydrolysis of the Zn^{2+} is significant in presence of metal excess and, therefore, does not consider the respective mass balance equations can alter the interpretation of potentiometric data.

Conclusion

This paper reports a study on the interactions between cysteine, penicilamine and glutathione and Pb^{2+} and Zn^{2+}, at different ionic strength and temperature.

The main conclusions can be summarized as follows:

- Potentiometric measurements evidenced similar speciation models for Pb^{2+}- c*ys*$^{2-}$ and -*psh*$^{2-}$ systems, with the formation of PbL^0, $PbLH^+$, $PbLH_2^{2+}$, $PbL(OH)^-$ and PbL_2^{2-} species.
- More complex is the speciation model for *gsh* systems, in particular for Zn^{2+}, with the formation of $Zn(gsh)^-$, $Zn(gsh)H^0$, $Zn(gsh)H_2^+$, $Zn(gsh)_2^{4-}$, $Zn(gsh)_2H^{3-}$ and $Zn(gsh)_2H_2^{2}$ species, together with the two mixed hydrolytic $Zn(gsh)OH^{3-}$ and $Zn(gsh)_2OH^{5-}$.
- Stability constants were determined at different ionic strengths ($0 \leq I \leq 1$ M) and temperatures ($15 \leq t \leq 45$ °C). From the dependence on ionic strength, formation constant values extrapolated at $I = 0$ mol·L^{-1} were calculated, together with parameters for the dependence on *I*. From the dependence on temperature, rough ΔH values were evaluated. The main contribution to the complexation free energy is entropic, with small enthalpic values.
- The knowledge of the parameters for the dependence on the ionic strength and temperature gives a complete thermodynamic picture of these systems, whose equilibrium constants can therefore be predicted for any experimental condition.
- For Pb^{2+} - *psh* and -*gsh* systems, UV spectrophotometric measurements were performed to confirm the speciation model and to define the UV spectral properties of these systems.
- The sequestering ability of the ligands towards Pb^{2+} and Zn^{2+} was evaluated by determining the $pL_{0.5}$ values, i.e. the total ligand concentration necessary to sequester 50% of the metal ion. All these ligands show good sequestering ability, in particular for Pb^{2+}-*cys* and -*psh* systems, $pL_{0.5}$ reaches the value of 8.24 and 9.01, respectively. The effect of temperature and ionic strength was evaluated.
- The data here collected will contribute to extend the database of thermodynamic parameters. This is fundamental for the modelling studies addressed to the formulation of highly descriptive semiempirical equations able to predict the

stability constant of a species under various experimental conditions (ionic strength, ionic medium, temperature) as well as to calculate the stability of species under hardly accessible experimental conditions.

References

1. G. Atmaca, *Yonsei Medical Journal*, 2004, **45**, 776-788.
2. P. Manna, J. Das and P. C. Sil, *Curr. Diabetes Rev.* , 2013, **9**, 237-248.
3. K. T. Brosnan and M. E. Brosnan, *J. Nutr.*, 2006, **136**, 1636S-1640S
4. S. Parcell, *Alternative Medicine Review*, 2002, **7**, 22-44.
5. A. E. Martell, R. M. Smith and R. J. Motekaitis, *Critically Selected Stability Constants of Metal Complexes. National Institute of Standard and Technology, NIST*, ed. PC-based Database, Gaithersburg, 2004.
6. L. Pettit and K. J. Powell, *The IUPAC Stability Constants Database*, ed. Academic Software, 2001.
7. P. M. May, D. Rowland, E. Königsberger and G. Hefter, *Talanta*, 2010, **81**, 142-148.
8. P. Cardiano, D. Cucinotta, C. Foti, O. Giuffrè and S. Sammartano, *J. Chem. Eng. Data*, 2011, **56**, 1995-2004.
9. P. Cardiano, C. De Stefano, O. Giuffrè and S. Sammartano, *Biophys. Chem.*, 2008, **133**, 19-27.
10. P. Cardiano, G. Falcone, C. Foti, O. Giuffrè and A. Napoli, *J. Inorg. Biochem.*, 2013, **129**, 84-93.
11. P. Cardiano, G. Falcone, C. Foti, O. Giuffrè and S. Sammartano, *New J. Chem.*, 2011, **35**, 800 - 806.
12. P. Cardiano, G. Falcone, C. Foti and S. Sammartano, *J. Chem. Eng. Data*, 2011, **56**, 4741-4750.
13. G. Falcone, C. Foti, A. Gianguzza, O. Giuffrè, A. Napoli, A. Pettignano and D. Piazzese, *Anal. Bioanal. Chem.*, 2013, **405**, 881-893.
14. C. Bretti, C. De Stefano, C. Foti, O. Giuffrè and S. Sammartano, *J. Solution Chem.*, 2009, **38**, 1225-1245.
15. P. Crea, A. De Robertis, C. De Stefano, D. Milea and S. Sammartano, *J. Chem. Eng. Data*, 2007, 1028-1036.
16. P. Cardiano, O. Giuffrè, A. Napoli and S. Sammartano, *New J. Chem.*, 2009, **33**, 2286-2295.
17. S. Materazzi, C. Foti, F. Crea, R. Risoluti and J. Finamore, *Thermochimica Acta*, 2014, **580**, 7-12.
18. C. A. McAuliffe, J. V. Quagliano and L. M. Vallarino, *Inorg. Chem.* , 1966, **5**, 1996-2003.
19. A. Dos Santos, I. C. Bellin, P. P. Corbi, A. Cuin, A. H. Rosa, M. Olimpia de O. Rezende, J. C. Rocha and P. Melnikov, *J. Braz. Chem. Soc.*, 2004, **15**, 437-440.
20. A. M. Corrie, M. L. D. Touche and D. R. Williams, *J. Chem. Soc. Dalton Trans.*, 1973, 2561-2565.
21. A. M. Corrie, M. D. Walker and D. R. Williams, *J. Chem. Soc. Dalton Trans.*, 1976, 1012-1015.
22. A. M. Corrie and D. R. Williams, *J. Chem. Soc. Dalton Trans.*, 1976, 1068-1072.
23. L. Ferretti, L. Elviri, M. A. Pellinghelli, G. Predieri and M. Tegoni, *J. Inorg. Biochem.*, 2007, **101**, 1442-1456.
24. A. Krezel, J. Wójcik, M. Maciejczyk and W. Bal, *Chem. Comm.*, 2003, 704-705.
25. C. Norman and R. A. Manning, *J. Am. Chem. Soc.*, 1955, **77**, 5225-5228.
26. M. L. D. Touche and D. R. Williams, *J. Chem. Soc. Dalton Trans.*, 1976, 1355-1359.

27. D. M. Templeton, F. Ariese, R. Cornelis, L. Danielsson, H. Muntau, H. P. van Leeuwen and R. Lobinski, *Pure Appl. Chem.*, 2000, **72**, 1453–1470.
28. C. De Stefano, S. Sammartano, P. Mineo and C. Rigano, Computer Tools for the Speciation of Natural Fluids, in *Marine Chemistry - An Environmental Analytical Chemistry Approach*, ed. A. Gianguzza, E. Pelizzetti and S. Sammartano, Kluwer Academic Publishers, Amsterdam, 1997, pp. 71-83.
29. P. Gans, A. Sabatini and A. Vacca, *Ann. Chim. (Rome)*, 1999, **89**, 45-49.
30. L. Alderighi , P. Gans, A. Ienco, D. Peters, A. Sabatini and A. Vacca, *Coord. Chem. Rev.*, 1999, **184**, 311-318.
31. C. F. Baes and R. E. Mesmer, *The hydrolysis of cations*, ed. John Wiley & Sons, New York, 1976.
32. K. J. Powell, P. L. Brown, R. H. Byrne, T. Gajda, G. Hefter, A. Leuz, S. Sjöberg and H. Wanner, *Pure Appl. Chem.*, 2009, **81**, 2425-2476.
33. A. Vacca, A. Sabatini and M. A. Gristina, *Coord. Chem. Rev.*, 1972, **8**, 45-53.
34. C. Bretti, C. De Stefano, C. Foti and S. Sammartano, *J. Solution Chem.*, 2006, **35**, 1227-1244.
35. C. Foti and S. Sammartano, *J. Chem. Eng. Data*, 2010, **55**, 904–911.
36. C. Bretti, F. Crea, C. De Stefano, C. Foti, S. Materazzi and G. Vianelli, *J. Chem. Eng. Data*, 2013, **58**, 2835-2847.
37. G. Falcone, C. Foti and S. Sammartano, *J. Chem. Eng. Data*, 2012, **57**, 3636−3643.
38. C. De Stefano, C. Foti, O. Giuffrè and S. Sammartano, *J. Mol. Liquid*, 2014, **195**, 9–16.
39. G. Falcone, O. Giuffrè and S. Sammartano, *J. Mol. Liquids*, 2011 **159**, 146-151.
40. G. Schwarzenbach and H. Flaschka, *Complexometric titrations*, ed. Methuen, London, 1969.
41. A. Gianguzza, O. Giuffrè, D. Piazzese and S. Sammartano, *Coord. Chem. Rev.*, 2012, **256**, 222-239.
42. G. Lenz and A. Martell, *Biochem.*, 1964, **3**, 745-750.

Table 1. Literature data on Pb^{2+}-*cys*, -*psh* and -*gsh* and on Zn^{2+}-*gsh* systems

M	**L**	**I /mol L^{-1}**	***t* /°C**	**logβ**	**Ref**
Pb^{2+}	*cys*	1 (NaClO$_4$)	25	12.20 (ML); 16.16 (MLH); 25.10(ML$_2$H); 2.04 (MLOH)	6
		0.5 (NaClO$_4$)	25	12.21 (ML)	6
		3 (NaClO$_4$)	25	12.21 (ML); 17.35 (MLH); 18.57 (ML$_2$); 27.48 (ML$_2$H); 7.33 (ML$_2$OH)	21
		3 (NaClO$_4$)	25	13.21 (ML); 17.43 (MLH); 27.30 (ML$_2$H)	22
		3 (NaClO$_4$)	25	13.36 (ML); 19.20 (MLH); 22.47 (MLH$_2$)	20
		0.15(KNO3)	25	12.20 (ML)	25
	psh	0.15 (NaCl)	37	13.06 (ML); 16.28 (MLH); 7.33 (MLOH)	5, 6
		3 (NaClO$_4$)	25	14.32 (ML); 17.72 (MLH); 19.05 (ML$_2$); 27.98 (ML$_2$H); 34.04 (ML$_2$H$_2$); 7.55 (ML$_2$OH)	21
		0.15 (KNO$_3$)	25	13.0 (ML); 17.30 (MLH)	6
	gsh	3 (NaClO$_4$)	25	10.57 (ML); 17.14 (MLH); 15.00 (ML$_2$); 24.66 (ML$_2$H); 32.10 (ML$_2$H$_2$); 4.50 (ML$_2$OH)	21
Zn^{2+}	*gsh*	0.15 (NaClO$_4$)	37	7.98 (ML); 14.11 (MLH); 12.48 (ML$_2$); 21.36 (ML$_2$H); 28.08 (ML$_2$H$_2$); -0.71 (MLOH); 3.12 (ML$_2$OH)	26
		3.0 (NaClO$_4$)	25	8.57 (ML); 14.76 (MLH); 13.59 (ML$_2$); 23.27(ML$_2$H); 30.62 (ML$_2$H$_2$); 3.59 (ML$_2$(OH)$_2$)	21
		0.1 (KNO$_3$)	25	8.31 (ML); 14.74 (MLH); 13.61 (ML$_2$); 22.53 (ML$_2$H); 29.50 (ML$_2$H$_2$); 3.81 (ML$_2$OH); -6.49 (ML$_2$(OH)$_2$)	24
		0.1 (KCl)	25	7.89 (ML); 14.21 (MLH); 12.39 (ML$_2$); 21.72 (ML$_2$H); 29.03 (ML$_2$H$_2$); 2.36 (ML$_2$OH); -8.58 (ML$_2$(OH)$_2$); 9.56 (M$_2$L$_2$OH); 0.15 (M$_2$L$_2$(OH)$_2$)	23

Table 2. Equilibrium constants for the formation of the hydrolytic species of Pb^{2+} and Zn^{2+} and the protonation of cys^{2-}, psh^{2-} and gsh^{3-}, at different ionic strengths and at t = 25 °C

Reaction	log β			Ref.
	I /mol L^{-1}			
	0.1	0.5	1	
$Pb^{2+} + H_2O = Pb(OH)^+ + H^+$	-7.67	-7.78	-7.81	32
$Pb^{2+} + 2\ H_2O = Pb(OH)_2^0 + 2\ H^+$	-17.14	-17.23	-17.24	
$Pb^{2+} + 3\ H_2O = Pb(OH)_3^- + 3\ H^+$	-28.06	-28.18	-28.33	
$3\ Pb^{2+} + 4\ H_2O = Pb_3(OH)_4^{2+} + 4\ H^+$	-23.41	-23.53	-23.48	
$4\ Pb^{2+} + 4\ H_2O = Pb_4(OH)_4^{4+} + 4\ H^+$	-20.13	-19.82	-19.64	
$6\ Pb^{2+} + 8\ H_2O = Pb_6(OH)_8^{4+} + 8\ H^+$	-42.86	-42.74	-42.60	
$2\ Pb^{2+} + H_2O = Pb_2(OH)^{3+} + H^+$	-7.08	-7.00	-7.00	
$Zn^{2+} + H_2O = Zn(OH)^+ + H^+$	-9.14	-9.15	-9.16	31
$Zn^{2+} + 2\ H_2O = Zn(OH)_2^0 + 2\ H^+$	-17.10	-17.1	-17.22	
$Zn^{2+} + 3\ H_2O = Zn(OH)_3^- + 3\ H^+$	-28.40	-28.40	-28.47	
$Zn^{2+} + 4\ H_2O = Zn(OH)_4^{2-} + 4\ H^+$	-40.80	-40.85	-40.38	
$2\ Zn^{2+} + H_2O = Zn_2(OH)^{3+} + H^+$	-8.70	-8.89	-8.89	
$2\ Zn^{2+} + 6\ H_2O = Zn_2(OH)_6^{2-} + 6\ H^+$	-57.50	-57.53	-57.32	
$H^+ + cys^{2-} = H(cys)^-$	10.46	10.28	10.26	11, 12
$2H^+ + cys^{2-} = H_2(cys)^0$	18.78	18.54	18.56	
$3H^+ + cys^{2-} = H_3(cys)^+$	21.04	20.68	20.54	
$H^+ + psh^{2-} = H(psh)^-$	10.40	10.34	10.42	12
$2H^+ + psh^{2-} = H_2(psh)^0$	18.21	18.19	18.39	
$3H^+ + psh^{2-} = H_3(psh)^+$	20.00	20.08	20.44	
$H^+ + gsh^{3-} = H(gsh)^{2-}$	9.50	9.30	9.30	10
$2H^+ + gsh^{3-} = H_2(gsh)^-$	18.20	17.85	17.88	
$3H^+ + gsh^{3-} = H_3(gsh)^0$	21.76	21.31	21.38	
$4H^+ + gsh^{3-} = H_4(gsh)^+$	23.94	23.49	23.62	

Table 3. Equilibrium constants for Pb^{2+} -cys^{2-}, -psh^{2-} and -gsh^{3-} (in $NaNO_3$) and for Zn^{2+}-gsh^{3-} systems (in NaCl) at different ionic strengths and at t = 25 °C

Reaction	log β		
	I /mol L^{-1}		
	0.1	0.5	1
$Pb^{2+} + \mathit{cys}^{2-} = Pb(\mathit{cys})^0$	13.12(2)[a)]	12.58(1)[a)]	12.16(3)[a)]
$Pb^{2+} + \mathit{cys}^{2-} + H^+ = Pb(\mathit{cys})H^+$	17.77(2)	17.21(1)	16.78(4)
$Pb^{2+} + \mathit{cys}^{2-} + 2H^+ = Pb(\mathit{cys})H_2^{2+}$	22.72(3)	22.28(3)	21.93(4)
$Pb^{2+} + 2\ \mathit{cys}^{2-} = Pb(\mathit{cys})_2^{2-}$	17.56(3)	17.00(3)	16.57(2)
$Pb^{2+} + \mathit{cys}^{2-} + H_2O = Pb(\mathit{cys})(OH)^- + H^+$	2.49(4)	2.09(5)	1.79(3)
$Pb^{2+} + \mathit{psh}^{2-} = Pb(\mathit{psh})^0$	13.37(2)	12.93(1)	12.66(2)
$Pb^{2+} + \mathit{psh}^{2-} + H^+ = Pb(\mathit{psh})H^+$	17.11(2)	16.84(2)	16.76(2)
$Pb^{2+} + \mathit{psh}^{2-} + 2H^+ = Pb(\mathit{psh})H_2^{2+}$	20.97(2)	20.99(3)	21.23(3)
$Pb^{2+} + 2\ \mathit{psh}^{2-} = Pb(\mathit{psh})_2^{2-}$	16.93(3)	16.66(2)	16.59(3)
$Pb^{2+} + \mathit{psh}^{2-} + H_2O = Pb(\mathit{psh})(OH)^- + H^+$	3.19(2)	2.74(2)	2.39(2)
$Pb^{2+} + \mathit{gsh}^{3-} = Pb(\mathit{gsh})^-$	9.67(2)	7.81(2)	6.60(2)
$Pb^{2+} + \mathit{gsh}^{3-} + H^+ = Pb(\mathit{gsh})H^0$	17.05(1)	15.75(1)	15.02(2)
$Pb^{2+} + \mathit{gsh}^{3-} + 2H^+ = Pb(\mathit{gsh})H_2^+$	22.14(2)	21.12(2)	20.69(3)
$Pb^{2+} + 2\ \mathit{gsh}^{3-} = Pb(\mathit{gsh})_2^{4-}$	15.48(7)	13.82(2)	12.30(3)
$Pb^{2+} + 2\ \mathit{gsh}^{3-} + H^+ = Pb(\mathit{gsh})_2H^{3-}$	24.51(4)	22.70(2)	21.42(3)
$Pb^{2+} + 2\ \mathit{gsh}^{3-} + 2H^+ = Pb(\mathit{gsh})_2H_2^{2-}$	32.59(2)	30.79(1)	29.82(2)
$Zn^{2+} + \mathit{gsh}^{3-} = Zn(\mathit{gsh})^-$	8.80(1)	8.00(1)	7.74(1)
$Zn^{2+} + \mathit{gsh}^{3-} + H^+ = Zn(\mathit{gsh})H^0$	15.21(1)	14.55(1)	14.51(1)
$Zn^{2+} + \mathit{gsh}^{3-} + 2\ H^+ = Zn(\mathit{gsh})H_2^+$	20.80(1)	19.87(1)	19.42(1)
$Zn^{2+} + 2\ \mathit{gsh}^{3-} = Zn(\mathit{gsh})_2^{4-}$	13.58(2)	12.57(1)	12.00(1)
$Zn^{2+} + 2\ \mathit{gsh}^{3-} + H^+ = Zn(\mathit{gsh})_2H^{3-}$	22.71(1)	21.59(1)	21.16(1)
$Zn^{2+} + 2\ \mathit{gsh}^{3-} + 2H+ = Zn(\mathit{gsh})_2H_2^{2-}$	29.80(1)	28.64(1)	28.39(1)
$Zn^{2+} + \mathit{gsh}^{3-} + H_2O = Zn(\mathit{gsh})(OH)^{2-} + H^+$	-0.26(1)	-1.05(1)	-1.47(1)
$Zn^{2+} + 2\mathit{gsh}^{3-} + H_2O = Zn(\mathit{gsh})_2(OH)^{5-} + H^+$	3.64(1)	2.65(2)	1.86(3)

[a)] Least-squares errors on last significant figure are shown in parenthesis.

Table 4. Equilibrium constants for Pb^{2+} -cys^{2-}, -psh^{2-} and -gsh^{3-} and Zn^{2+}-gsh^{3-}systems at infinite dilution (log β^0), together with C parameter for the ionic strength dependence (eq. 1), at t = 25 °C

Reaction	log β^0	z*	C
$Pb^{2+} + \mathit{cys}^{2-} = Pb(\mathit{cys})^0$	13.96(5) [a]	8	-0.23(7) [a][b]
$Pb^{2+} + \mathit{cys}^{2-} + H^+ = Pb(\mathit{cys})H^+$	18.61(6)	8	-0.27(6)
$Pb^{2+} + \mathit{cys}^{2-} + 2H^+ = Pb(\mathit{cys})H_2^{2+}$	23.36(6)	6	-0.25(6)
$Pb^{2+} + 2\ \mathit{cys}^{2-} = Pb(\mathit{cys})_2^{2-}$	18.40(6)	8	-0.27(6)
$Pb^{2+} + \mathit{cys}^{2-} + H_2O = Pb(\mathit{cys})(OH)^- + H^+$	3.11(9)	6	-0.15(6)
$Pb^{2+} + \mathit{psh}^{2-} = Pb(\mathit{psh})^0$	14.17(1)	8	0.05(6)
$Pb^{2+} + \mathit{psh}^{2-} + H^+ = Pb(\mathit{psh})H^+$	17.88(2)	8	0.44(6)
$Pb^{2+} + \mathit{psh}^{2-} + 2H^+ = Pb(\mathit{psh})H_2^{2+}$	21.48(3)	6	0.92(5)
$Pb^{2+} + 2\ \mathit{psh}^{2-} = Pb(\mathit{psh})_2^{2-}$	17.70(3)	8	0.46(6)
$Pb^{2+} + \mathit{psh}^{2-} + H_2O = Pb(\mathit{psh})(OH)^- + H^+$	3.83(2)	6	-0.26(5)
$Pb^{2+} + \mathit{gsh}^{3-} = Pb(\mathit{gsh})^-$	11.03(3)	12	-1.9(1)
$Pb^{2+} + \mathit{gsh}^{3-} + H^+ = Pb(\mathit{gsh})H^0$	18.66(3)	14	-0.75(3)
$Pb^{2+} + \mathit{gsh}^{3-} + 2H^+ = Pb(\mathit{gsh})H_2^+$	23.69(3)	14	-0.15(4)
$Pb^{2+} + 2\ \mathit{gsh}^{3-} = Pb(\mathit{gsh})_2^{4-}$	16.43(3)	6	-2.94(7)
$Pb^{2+} + 2\ \mathit{gsh}^{3-} + H^+ = Pb(\mathit{gsh})_2H^{3-}$	26.06(3)	14	-1.83(7)
$Pb^{2+} + 2\ \mathit{gsh}^{3-} + 2H^+ = Pb(\mathit{gsh})_2H_2^{2-}$	34.79(1)	20	-0.85(4)
$Zn^{2+} + \mathit{gsh}^{3-} = Zn(\mathit{gsh})^-$	10.09(7)	12	0.09(9) [c]
$Zn^{2+} + \mathit{gsh}^{3-} + H^+ = Zn(\mathit{gsh})H^0$	16.67(6)	14	0.69(8)
$Zn^{2+} + \mathit{gsh}^{3-} + 2\ H^+ = Zn(\mathit{gsh})H_2^+$	22.34(4)	14	-0.06(6)
$Zn^{2+} + 2\ \mathit{gsh}^{3-} = Zn(\mathit{gsh})_2^{4-}$	14.29(9)	6	-1.1(1)
$Zn^{2+} + 2\ \mathit{gsh}^{3-} + H^+ = Zn(\mathit{gsh})_2H^{3-}$	24.24(8)	14	-0.2(1)
$Zn^{2+} + 2\ \mathit{gsh}^{3-} + 2H+ = Zn(\mathit{gsh})_2H_2^{2-}$	31.92(7)	20	0.5(1)
$Zn^{2+} + \mathit{gsh}^{3-} + H_2O = Zn(\mathit{gsh})OH^{2-} + H^+$	0.65(7)	8	-0.5(1)
$Zn^{2+} + 2\ \mathit{gsh}^{3-} + H_2O = Zn(\mathit{gsh})_2OH^{5-} + H^+$	3.3(1)	-4	-2.4(1)

[a] Least-squares errors on last significant figure are shown in parenthesis, [b] in $NaNO_3$, [c] in NaCl.

Table 5. Equilibrium constants for Pb^{2+}-gsh^{3-} (in $\mathrm{NaNO_3}$) and Zn^{2+}-gsh^{3-} (in NaCl) system, at different temperatures and $I = 0.1$ mol L^{-1}

Reaction	log β			
	t /°C			
	15	25	37	45
$\mathrm{Pb}^{2+} + gsh^{3-} = \mathrm{Pb}(gsh)^{-}$	10.14(3) [a]	9.67(2) [a]	8.82(7) [a]	9.31(8) [a]
$\mathrm{Pb}^{2+} + gsh^{3-} + \mathrm{H}^{+} = \mathrm{Pb}(gsh)\mathrm{H}^{0}$	17.51(1)	17.05(1)	16.53(3)	16.78(2)
$\mathrm{Pb}^{2+} + gsh^{3-} + 2\mathrm{H}^{+} = \mathrm{Pb}(gsh)\mathrm{H_2}^{+}$	22.58(1)	22.14(2)	21.96(3)	21.98(3)
$\mathrm{Pb}^{2+} + 2\ gsh^{3-} = \mathrm{Pb}(gsh)_2{}^{4-}$	16.16(8)	15.48(7)	14.77(8)	15.78(3)
$\mathrm{Pb}^{2+} + 2\ gsh^{3-} + \mathrm{H}^{+} = \mathrm{Pb}(gsh)_2\mathrm{H}^{3-}$	25.05(4)	24.51(4)	23.19(1)	24.21(3)
$\mathrm{Pb}^{2+} + 2\ gsh^{3-} + 2\mathrm{H}^{+} = \mathrm{Pb}(gsh)_2\mathrm{H_2}^{2-}$	33.29(1)	32.59(2)	31.46(6)	31.85(2)
$\mathrm{Zn}^{2+} + gsh^{3-} = \mathrm{Zn}(gsh)^{-}$	8.90(1)	8.83(1)	8.74(2)	8.94(3)
$\mathrm{Zn}^{2+} + gsh^{3-} + \mathrm{H}^{+} = \mathrm{Zn}(gsh)\mathrm{H}^{0}$	15.42(2)	15.24(2)	15.02(5)	15.18(9)
$\mathrm{Zn}^{2+} + gsh^{3-} + 2\ \mathrm{H}^{+} = \mathrm{Zn}(gsh)\mathrm{H_2}^{+}$	21.22(2)	20.83(2)	20.42(2)	20.41(2)
$\mathrm{Zn}^{2+} + 2\ gsh^{3-} = \mathrm{Zn}(gsh)_2{}^{4-}$	13.56(7)	13.57(5)	13.30(6)	13.73(5)
$\mathrm{Zn}^{2+} + 2\ gsh^{3-} + \mathrm{H}^{+} = \mathrm{Zn}(gsh)_2\mathrm{H}^{3-}$	23.04(2)	22.73(2)	22.27(2)	22.46(3)
$\mathrm{Zn}^{2+} + 2\ gsh^{3-} + 2\mathrm{H}+ = \mathrm{Zn}(gsh)_2\mathrm{H_2}^{2-}$	30.40(2)	29.85(2)	29.27(2)	29.22(3)
$\mathrm{Zn}^{2+} + gsh^{3-} + \mathrm{H_2O} = \mathrm{Zn}(gsh)\mathrm{OH}^{2-} + \mathrm{H}^{+}$	-0.34(2)	-0.21(2)	-0.01(2)	0.45(3)
$\mathrm{Zn}^{2+} + 2\ gsh^{3-} + \mathrm{H_2O} = \mathrm{Zn}(gsh)_2\mathrm{OH}^{5-} + \mathrm{H}^{+}$	3.44(2)	3.63(2)	3.56(2)	4.20(3)

[a] Least-squares errors on last significant figure are shown in parenthesis.

Table 6. Overall and stepwise thermodynamic formation parameters for Pb^{2+}-gsh^{3-} (in $NaNO_3$) and Zn^{2+}-gsh^{3-} (in NaCl) system, at different temperatures and $I = 0.1$ mol L^{-1}

Reaction ($L = gsh^{3-}$)	-ΔG a)b)	ΔH a)b)	TΔS a)b)
$Pb^{2+} + L = PbL^-$	55.2(1)	-43(3)	12(3)
$Pb^{2+} + L + H^+ = PbLH^0$	97.32(6)	-55(3)	42(3)
$Pb^{2+} + L + 2H^+ = PbLH_2^+$	126.4(1)	-64(2)	62(2)
$Pb^{2+} + 2 L^{3-} = PbL_2^{4-}$	88.4(4)	-25(3)	63(3)
$Pb^{2+} + 2 L^{3-} + H^+ = PbL_2H^{3-}$	139.9(2)	-53(3)	87(3)
$Pb^{2+} + 2 L^{3-} + 2H^+ = PbL_2H_2^{2-}$	186(1)	-75(2)	111(2)
$Zn^{2+} + L^{3-} = ZnL^-$	50.23(6)	-1(5)	49(5)
$Zn^{2+} + L^{3-} + H^+ = ZnLH^0$	86.82(6)	-18(5)	69(5)
$Zn^{2+} + L^{3-} + 2 H^+ = ZnLH_2^+$	118.73(6)	-50(5)	69(5)
$Zn^{2+} + 2 L^{3-} = ZnL_2^{4-}$	77.5(1)	2(5)	80(5)
$Zn^{2+} + 2 L^{3-} + H^+ = ZnL_2H^{3-}$	129.63(6)	-40(6)	90(6)
$Zn^{2+} + 2 L^{3-} + 2H+ = ZnL_2H_2^{2-}$	170.10(6)	-73(5)	97(5)
$Zn^{2+} + L^{3-} + H_2O = ZnLOH^{2-} + H^+$	-1.48(6)	42(6)	41(6)
$Zn^{2+} + 2 L^{3-} + H_2O = ZnL_2OH^{5-} + H^+$	20.78(6)	35(6)	56(6)
$Pb^{2+} + L^{3-}$	55.2	-43	12
$Pb^{2+} + HL^{2-}$ c)	43.4	-18	25
$Pb^{2+} + H_2L^-$	23.5	4	28
$PbL^- + L^{3-}$	34.3	18	52
$PbL^- + HL^{2-}$	30.0	27	57
$PbL^- + H_2L^-$	26.7	37	63
$Zn^{2+} + L^{3-}$	50.2	-1	49
$Zn^{2+} + HL^{2-}$	32.6	19	51
$Zn^{2+} + H_2L^-$	14.8	20	35
$ZnL^- + L^{3-}$	27.3	3	30
$ZnL^- + HL^{2-}$	25.2	-2	23
$ZnL^- + H_2L^-$	16.0	-2	14
$Zn(OH)^+ + L^{3-}$	50.7	42	93
$ZnLOH^{2-} + L^{3-}$	22.3	-7	15

a) In kJ mol^{-1}; b) least-squares errors on last significant figure are shown in parenthesis; c) ΔH for HL and H_2L formation from ref. 13.

Table 7. Conditional formation constants for Pb^{2+} -psh^{2-} and -gsh^{3-} systems obtained by UV spectrophotometry and potentiometry, at different pH values and t = 25 °C

pH	$\log K_{cond}$			
	psh		*gsh*	
	UV	ISE-H^+	UV	ISE-H^+
5	3.10	3.13	2.45	1.95
6	4.97	5.01	2.66	2.67
7	6.87	6.92	3.60	3.65
8	8.03	8.04	4.78	4.54
8.5	8.31	8.25	5.22	4.92

Table 8. $pL_{0.5}$ values of *cys*, *psh* and *gsh* towards different metal and organometallic cations, at different experimental conditions

L	I [a)]	t [b)]	pH	$pL_{0.5}$					
				Pb^{2+}	Zn^{2+}	Hg^{2+} [c)]	CH_3Hg^+ [d)]	$(CH_3)_2Sn^{2+}$ [e)]	$(CH_3)_3Sn^+$ [e)]
cys	0.1	25	7	8.2	5.7[f)]	23.5	11.6	-	-
psh	0.1	25	7	9.0	7.2[f)]	22.8	11.2	-	-
gsh	0.1	25	7	5.9	4.7	20.7	11.4	3.5	2.6
gsh	0.1	37	7	5.8	5.1				
gsh	1	25	7	4.3	4.1				
gsh	0.1	25	5	4.2	2.7				

[a)] In mol L^{-1}; [b)] in °C; [c)] Ref. 12; [d)] Ref. 11, 13; [e)] Ref. 10; [f)] calculated by data of ref. 42.

2-Amino-3-sulfhydrylpropanoic acid
(Cysteine, H_2*cys*)

(2*S*)-2-amino-3-methyl-3-sulfanyl-butanoic acid
(*Penicillamine*, H_2*psh*)

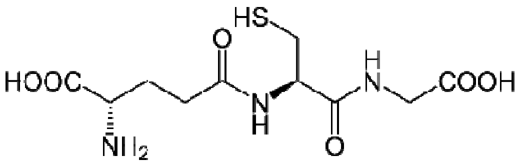

2-Amino-5-[[1-[(carboxymethylamino)-1-oxo-3-sulfanylpropan-2-yl]amino]-5-oxopentanoic acid (*Glutathione*, H_3*gsh*)

Fig. 1. Structure formula of ligands

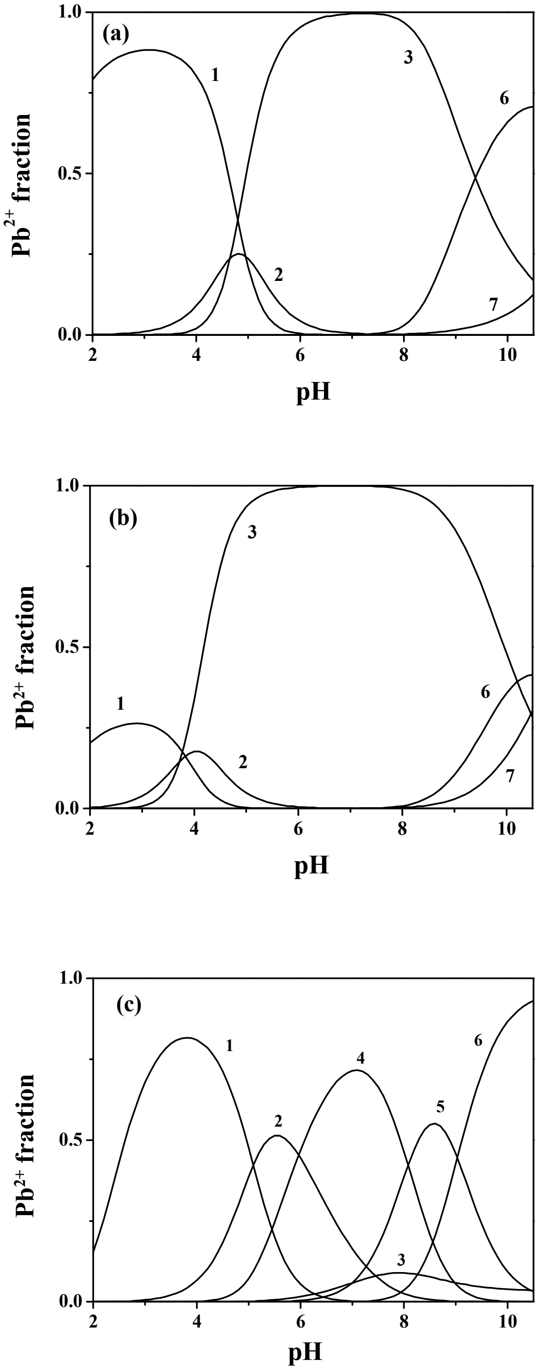

Fig. 2. Speciation diagrams for (a) Pb^{2+} -*cys*$^{2-}$, (b) -*psh*$^{2-}$ and (c) -*gsh*$^{3-}$ systems.
Experimental conditions: C_M = 1 mmol L^{-1}, C_L = 2 mmol L^{-1}, I = 0.1 mol L^{-1} ($NaNO_3$) t = 25 °C
Species: 1. MLH_2, 2. MLH, 3. ML, 4. ML_2H_2, 5. ML_2H, 6. ML_2, 7. MLOH.

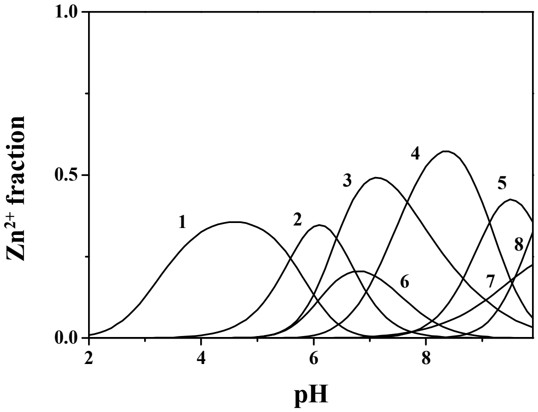

Fig. 3. Speciation diagrams for Zn^{2+}-*gsh*$^{3-}$ system. Experimental conditions: C_{Zn} = 1 mmol L^{-1}, C_{gsh} = 2 mmol L^{-1}, I = 0.1 mol L^{-1} (NaCl), t = 25 °C

Species: 1. MLH_2, 2. MLH, 3. ML, 4. ML_2H, 5. ML_2, 6. ML_2H_2, 7. MLOH, 8. ML_2OH.

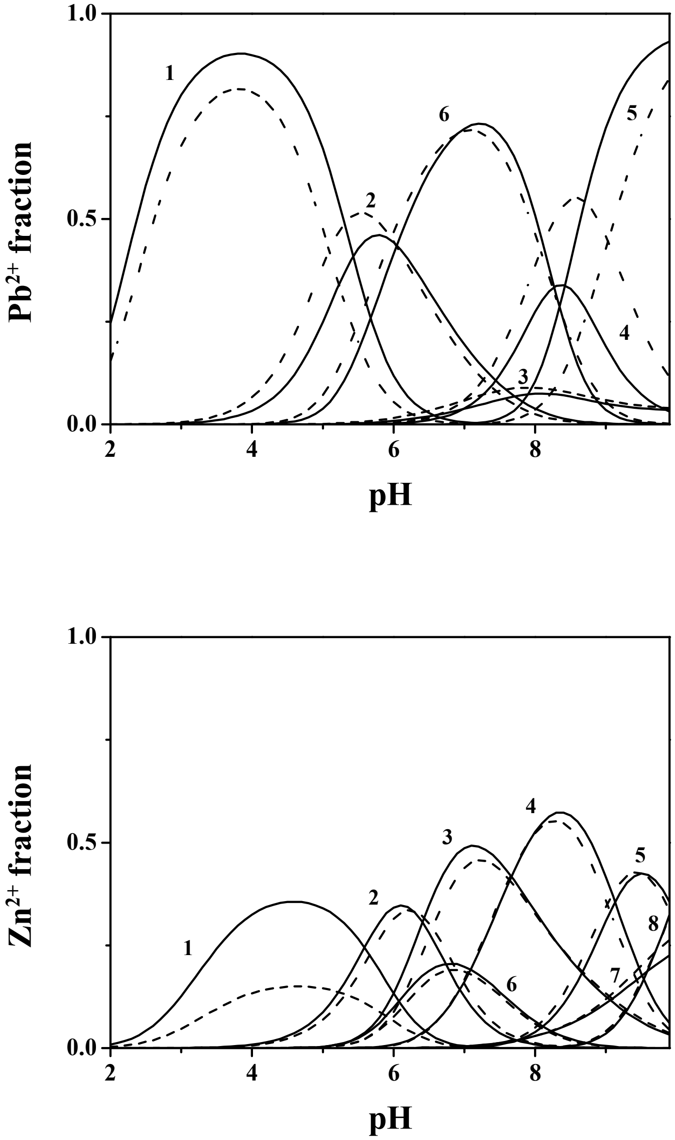

Fig. 4. Speciation diagram for Pb^{2+}-gsh^{3-} (in $NaNO_3$) and Zn^{2+}-gsh^{3-} (in NaCl) systems a $I = 0.1$ mol L^{-1}; $t = 25$ °C (dotted lines) and $t = 37$ °C (full lines).

Experimental conditions: $C_M = 1$ mmol L^{-1}; $C_{gsh} = 2$ mmol L^{-1}.

Species: 1. MLH_2, 2. MLH, 3. ML; 4. ML_2H, 5. ML_2, 6. ML_2H_2, 7. MLOH, 8. ML_2OH.

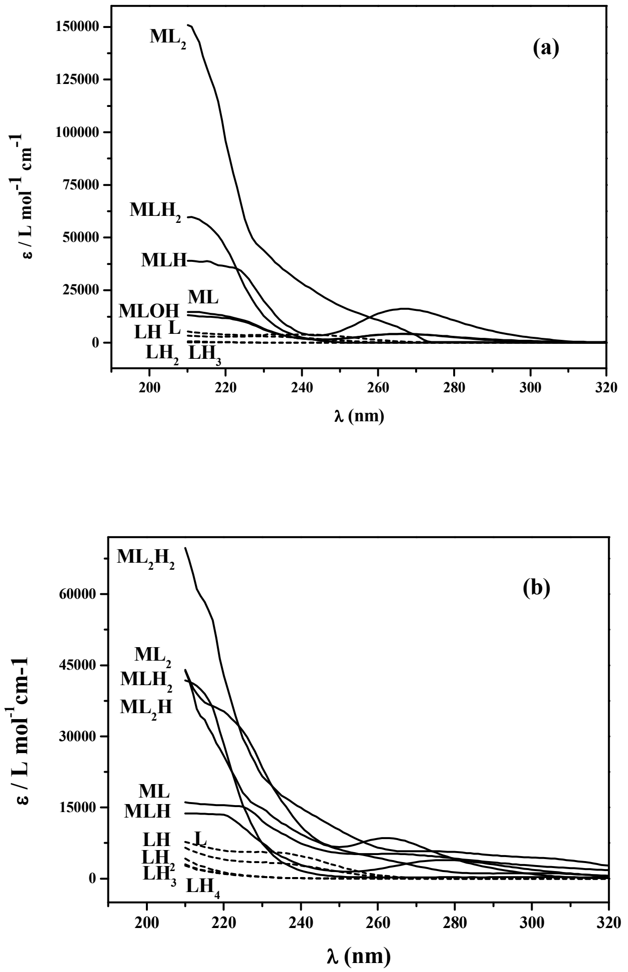

Fig. 5 Molar absorbances of (a) Pb^{2+}-*psh*$^{2-}$ and (b) Pb^{2+}-*gsh*$^{3-}$ species, at *t* = 25 °C and *I* = 0.006 mol L^{-1}.

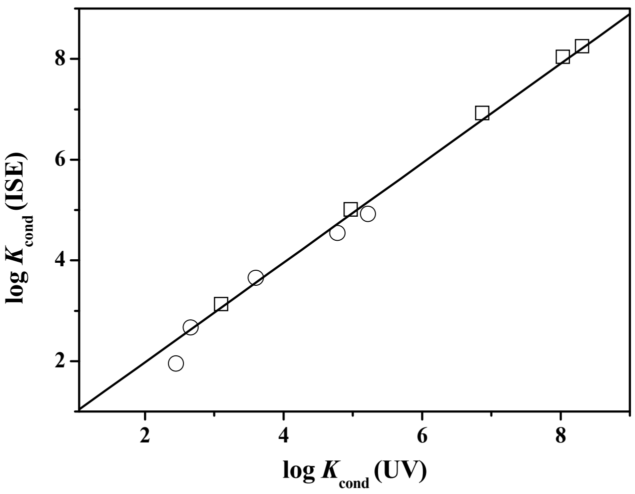

Fig. 6. Conditional formation constants calculated by potentiometric data *vs.* those by spectrophotometric ones, for (□) Pb^{2+}-*psh* and (O) Pb^{2+}-*gsh* systems.

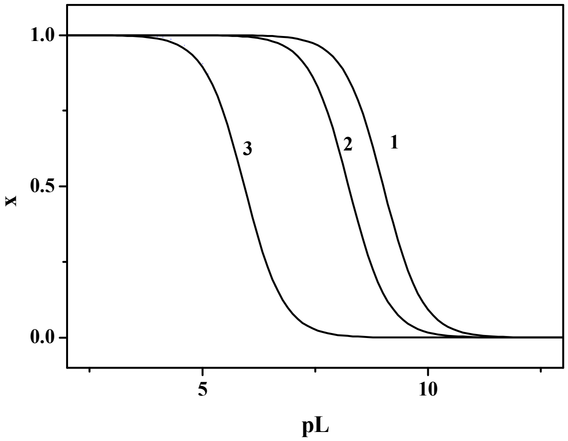

Fig. 7 Sequestering ability of (1) *psh*, (2) *cys* and (3) *gsh* towards Pb^{2+} at I = 0.1 mol L^{-1}, t = 25 °C and pH = 7.

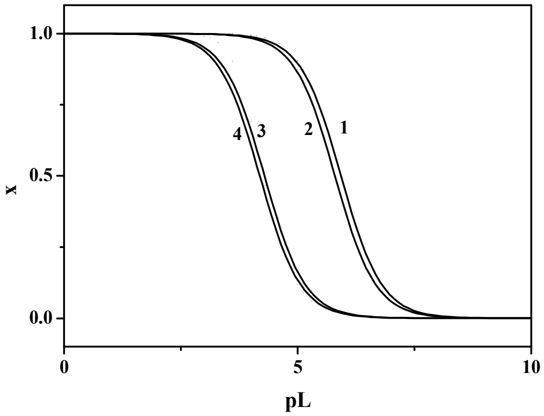

Fig. 8 Sequestering ability of *gsh* towards Pb^{2+} at different experimental conditions

1. $I = 0.1$ mol L^{-1}, $t = 25$ °C, pH = 7
2. $I = 0.1$ mol L^{-1}, $t = 37$ °C, pH = 7
3. $I = 0.1$ mol L^{-1}, $t = 25$ °C, pH = 5
4. $I = 1$ mol L^{-1}, $t = 25$ °C, pH = 7

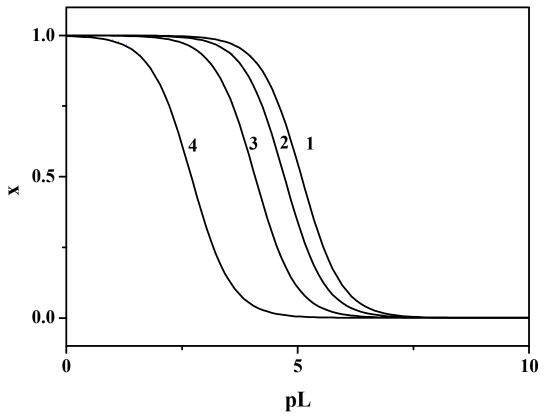

Fig. 9 Sequestering ability of *gsh* towards Zn^{2+} at different experimental conditions

1. I = 0.1 mol L^{-1}, t = 37 °C, pH = 7
2. I = 0.1 mol L^{-1}, t = 25 °C, pH = 7
3. I = 1 mol L^{-1}, t = 25 °C, pH = 7
4. I = 0.1 mol L^{-1}, t = 25 °C, pH = 5